

RESEARCH

Open Access



An adaptive task scheduling algorithm for 3-D target imaging in radar network

Dan Wang¹, Qun Zhang^{1,2*}, Ying Luo^{1,2}, Xiaowen Liu³ and Jia Liang¹

*Correspondence:

afeuzq@163.com

¹ The Institute of Information and Navigation, Air Force Engineering University, Xi'an 710077, China

Full list of author information is available at the end of the article

Abstract

An effective task scheduling method is the premise and guarantee for cooperative imaging in radar network. In this article, an adaptive task scheduling algorithm for three-dimensional (3-D) target imaging in radar network is investigated. The aim of our strategy is to achieve the multiple 3-D target imaging tasks with the minimal task time. Firstly, the 3-D target image can be reconstructed by high-resolution inverse imaging aperture radar (ISAR) images from three views, and the sparse imaging algorithm based on compressed sensing (CS) is adopted to acquire the ISAR images of the targets. Then, the adaptive task scheduling optimization model is constructed. Through the steps of target Information perception, radar selection and adjustment of imaging terminal time, the optimal task scheduling strategy is obtained and the resource utilization of radar network is significantly improved. Finally, the experiments highlight the effectiveness of our proposed task scheduling method.

Keywords: ISAR, 3-D target image, Adaptive task scheduling strategy, Radar network

1 Introduction

Radar, as an electronic sensor, plays an important role in the civilian and military fields because of its all weather, all day and certain penetrating capabilities [1]. A multi-static radar network, which is constituted of multiple dispersed radars, has the ability to achieve a wider range of detection and monitoring by information fusion. In addition, reasonable task scheduling method guarantees the cooperative work and can fully improve the overall performance the radar network.

High-resolution inverse synthetic aperture radar (ISAR) imaging technology that can acquire the target structure information becomes more and more popular in recent years [2–5]. An ISAR image can be obtained through long-term continuous observation and rich structure information such as shape, volume and surface physical parameters can be extracted for subsequent target classification and recognition. In fact, ISAR images are the two-dimensional (2-D) projection of the target scattering characteristics on the imaging projection plane (IPP). Due to the existence of anisotropy, the ISAR images from different observation views are not the same even for the same target. This brings great difficulty to target recognition. Thus, a three-dimensional (3-D) target image is regarded as a feasible solution to such a problem

[6–8]. One possible way to construct the 3-D target scattering distribution is to use the differences in ISAR images from multiple views in multi-static radar network [9]. Obviously, high-resolution ISAR images are the prerequisite for 3-D target imaging. According to the ISAR imaging principle, high-resolution ISAR images of the target require long-term continuous observation. Thus, there are many restrictions and conflicts on resource allocation when performing multiple types of tasks and the radar resource utilization will be greatly reduced. In addition, when the radar network has to deal with multiple targets appeared in the monitoring region, it is difficult to allocate enough observation time for each target. Thus, research on the task scheduling problem for 3-D multi-target imaging in radar network is essential and necessary.

Recent years, researchers show great interests on the problem of task scheduling in radar networks [10–16]. Motivated by better exploiting the limited system resource of radar network for target tracking, Yan proposed a joint detection and power allocation method [10]. An auction-based task scheduling method for multifunction radar network was investigated to maximize the whole revenue considering the timeliness constrained tasks [11]. Aiming at maximizing the power density of multiple regions for interference simultaneously, Zhang et al. proposed an antenna optimization deployment method in multi-static radar and numerical results were provided to demonstrate the validity [12]. In [13], Zhang proposed a power allocation optimization algorithm for a multi-static MIMO radar network in the case of multi-regional interference.

Note that, the current work mainly focuses on searching task, tracking task, anti-jamming task, etc., while few work involves the imaging task. In our previous work, we have proposed several game-theoretic-based task allocation methods for ISAR imaging in radar network [17, 18]. However, the task scheduling problem for multi-target 3-D imaging is much more complicated and the previous work cannot be directly applied to the problem. Therefore, a new task scheduling optimization model should be analyzed for the multi-target 3-D imaging problem. To the best of authors' knowledge, no literature has addressed the task scheduling problem of multi-target 3-D imaging in radar network.

In this article, an adaptive task scheduling algorithm for multi-target 3-D imaging is proposed. Firstly, a 3-D target imaging algorithm via multi-view ISAR images in radar network is analyzed. A sparse ISAR imaging algorithm is utilized to obtain the 2-D ISAR images and a 3-D target image is constructed based on the three ISAR images of different views. This cognitive imaging method leaves the possibility of adaptive task scheduling in radar network. Due to the cognition of target information, the multi-target 3-D imaging task is optimally scheduled according to further imaging requirements and the imaging terminal time can be adaptively adjusted. As a consequence, the multi-target 3-D imaging task is accomplished efficiently with the minimal task time, meanwhile the overall radar resource utilization is significantly improved.

The remainder of this article unfolds as follows. Section 2 introduces the 3-D target imaging method via radar network and formulates task scheduling problem. Section 3 details the whole flow of our proposed task scheduling strategy and Sect. 4 conducts the performance analysis on simulated experiments. Finally, Sect. 5 concludes this article.

2 Three-dimensional target imaging via radar network and task scheduling problem formulation

2.1 Imaging geometry of 3-D image via radar network

As known to all, a radar can obtain high-resolution profile in the range direction through transmitting signals with a large bandwidth. Meanwhile, a radar can obtain high-resolution profile of the azimuth direction through a bigger angle that the target rotates relative to the radar (i.e., longer synthetic aperture time). Consequently, after performing range compression and coherent processing, a high-resolution ISAR image in range and azimuth direction can be obtained for subsequent identification with enough radar observation time resource.

In essence, ISAR images can be seen as the 2-D projection of the target scattering characteristics on the imaging projection plane (IPP). The range direction and azimuth direction are considered as the two axes of IPP. When IPP varies, the ISAR images may be different even for the same target considering the anisotropy of the targets. This brings great difficulty to auto-target recognition.

Generally speaking, a 3-D target image which represents the 3-D scattering distribution of the target contains much more structure information of the target compared with 2-D ISAR images. Thus, a 3-D target image which can support target recognition better can be regarded as a feasible solution to such a problem. Radar network can be recognized as an efficient way to obtain the 3-D target image.

Specifically, in radar network, when the target is observed by several radars from different views, the observation information will be achieved simultaneously. Obviously, for each target, the 2-D ISAR images are obtained with certain differences by each radar. Considering the relationship between the ISAR images and the scattering distribution of the target, it is possible to construct the 3-D target image based on the differences between ISAR images [9].

Moreover, the geometry model for projection process by a single radar observation is shown in Fig. 1, where R represents the radar position and (R, X, Y, Z) represents a local

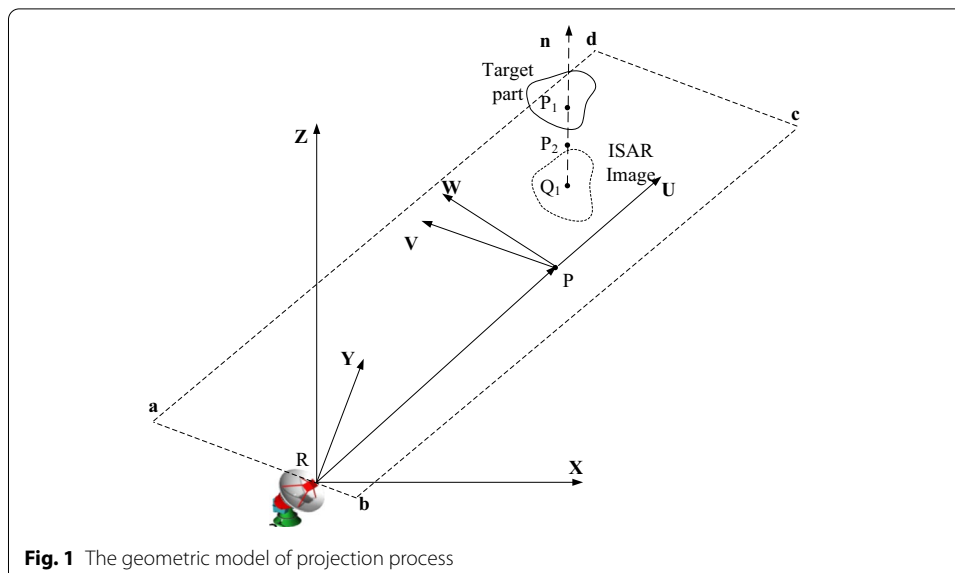


Fig. 1 The geometric model of projection process

Cartesian coordinate. Assume that point P denotes the center point of a target, which can be estimated by tracking algorithm, and point P is usually considered as the reference point for ISAR imaging. Additionally, (P, U, W) represents the coordinate system of IPP $abcd$, where axis U and W signify the directions of range and azimuth, respectively. \mathbf{n}_u and \mathbf{n}_w represent the unit vectors of axis U and W , respectively.

Let P_i denotes the spatial points, and Q_i denotes its projection onto IPP $abcd$. The projecting operation of P_i can be expressed as

$$\begin{cases} (\overrightarrow{PP_i} - \overrightarrow{PQ_i})^T \mathbf{n}_u = 0 \\ (\overrightarrow{PP_i} - \overrightarrow{PQ_i})^T \mathbf{n}_w = 0 \end{cases} \quad (1)$$

Assuming that $\overrightarrow{PQ_i} = u\mathbf{n}_u + w\mathbf{n}_w$, then the formula (1) is reformulated as

$$\mathbf{D}^T (\overrightarrow{PP_i} - \mathbf{D} \begin{bmatrix} u \\ w \end{bmatrix}) = 0, \quad \mathbf{D} = [\mathbf{n}_u, \mathbf{n}_w] \quad (2)$$

Thus, the coordinates of the projection point Q_i in (P, U, W) can be determined by

$$\begin{bmatrix} u \\ w \end{bmatrix} = (\mathbf{D}^T \mathbf{D})^{-1} \mathbf{D}^T \overrightarrow{PP_i} = \mathbf{F}_m(\overrightarrow{PP_i}) \quad (3)$$

where $\overrightarrow{PP_i} = \overrightarrow{RP_i} - \overrightarrow{RP}$ and $\mathbf{F}_m(\cdot)$ represents the projection operator for the m th radar that map the spatial points to the imaging projection plane.

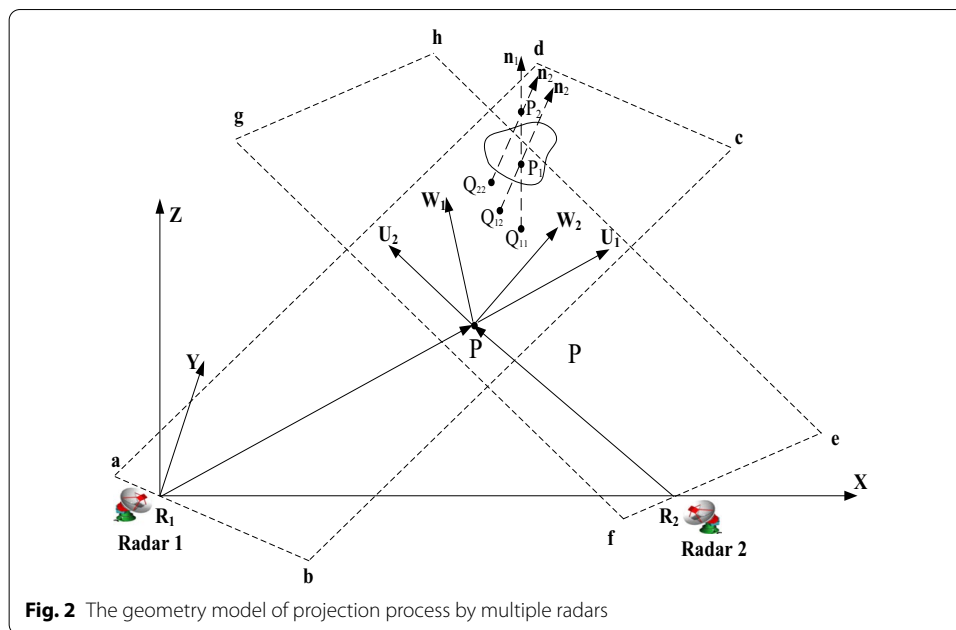
As mentioned above, the projection of a scatter point of the target to the plane $abcd$ will coincide with a point of an ISAR image. Consequently, if Q_i is coincides with a point of the ISAR image, point P_i can be regarded as one of the scattering points of the target with high probability. Then, a 3-D target image is constructed by collecting the approximate spatial points.

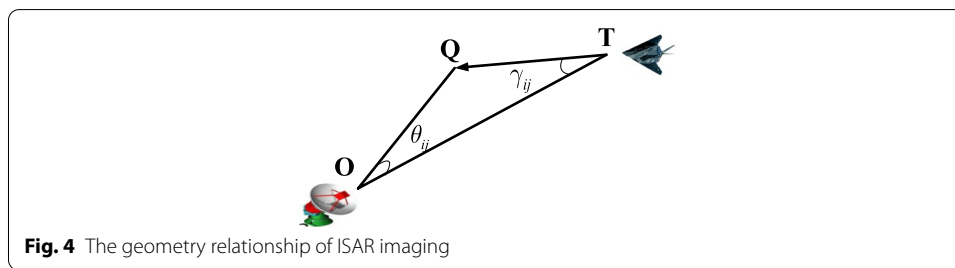
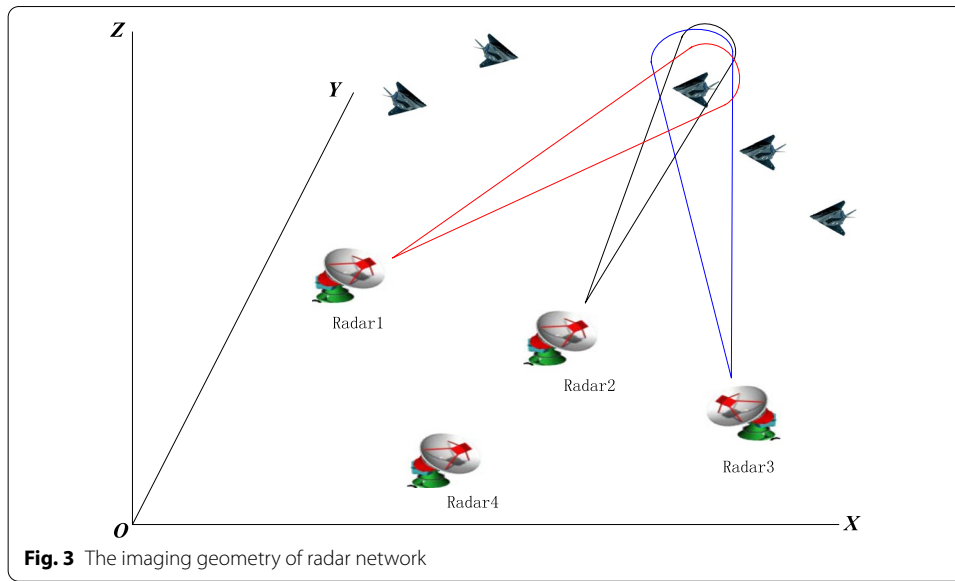
However, any spatial points parallel to the normal vector \mathbf{n} of plane $abcd$ should be projected to the same point. As illustrated in Fig. 1, the points P_1 and P_2 are two spatial points with same projection Q_1 on plane $abcd$. In fact, only point P_1 is the real scatter of the target. To overcome the problem of false points, multi-view observation in radar network is effective. For points P_1 and P_2 with the same projection Q_{11} on plane $abcd$, their projection on the imaging projection $efgh$ is separated as Q_{12} and Q_{22} , as illustrated in Fig. 2. Thus, the 3-D target image can be constructed with more additional information from different radars.

In addition, with the purpose of minimizing the difference between the ISAR images and the projection images using the least amount of spatial points, the reconstruction model of 3-D target image can be determined by

$$\min \omega \cdot \sum_{z=1}^{N_c} \sum_{y=1}^{N_c} \sum_{x=1}^{N_c} \mathbf{T}(x, y, z) + \sum_{m=1}^M \|\mathbf{F}_m(\mathbf{T}) - \mathbf{I}_m\|_2 \quad (4)$$

where the space containing all scattering points of the target is described by a three-dimensional grid model. N_c represents the number of the cells for each side of the space grid model and the 3-D matrix \mathbf{T} represents the value of the space grid model where contains only 1 and 0. $\mathbf{T}(x, y, z) = 1$ means there exists a spatial point in the correspond grid





reconstructed algorithms for formula (4). Neglecting the influence of reconstruction algorithms, this article focuses on the relationship between the quality of ISAR images and radar resources.

Resolution is an important indicator for evaluating the image quality. As known to all, the range resolution of ISAR images is determined by the radar signal bandwidth and is generally regarded as a constant. Additionally, as depicted in Fig. 4, the azimuth resolution of an ISAR image of the j th target ρ_a^j can be calculated as

$$\rho_a^j = \lambda / (2\theta_{ij}) \quad (5)$$

where λ represents the radar signal bandwidth and θ_{ij} represents the rotation angle. The points O, T, Q represent the location of the radar, the location of the imaging initial time and the location of the imaging terminal time of the target, respectively.

To summarize, the high resolution in azimuth direction requires a bigger rotation angle θ_{ij} , which means a longer synthetic aperture time (i.e., a longer task time). According to the geometry relationship of ISAR imaging as illustrated in Fig. 4, the distance $|\mathbf{R}_{QT}|$ that the target flies during the imaging process can be calculated by

$$|\mathbf{R}_{QT}| = \frac{|\mathbf{R}_{OT}| \cdot \sin(\theta_{ij})}{\sin(\pi - \theta_{ij} - \gamma_{ij})} \quad (6)$$

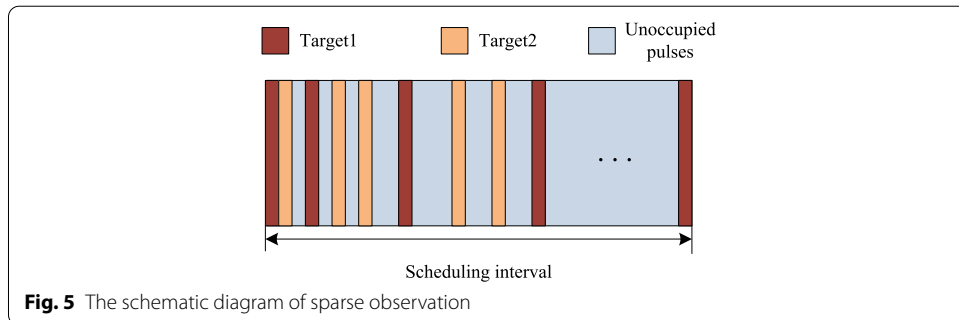
Then, the synthetic aperture time t_{ij} that the i th target is imaged by the j th radar be determined by

$$t_{ij} = \frac{|\mathbf{R}_{QT}|}{|\mathbf{V}_j|} = \frac{|\mathbf{R}_{OT}| \cdot \sin\left(\frac{\lambda}{2\rho_a^j}\right)}{\sin\left(\arccos\left(\frac{\mathbf{R}_{OT} \cdot \mathbf{V}_j}{|\mathbf{R}_{OT}| \cdot |\mathbf{V}_j|}\right) + \frac{\lambda}{2\rho_a^j}\right) \cdot |\mathbf{V}_j|} \quad (7)$$

where \mathbf{V}_j and \mathbf{R}_{OT} represent the speed vector of the j th target and the distance vector at the imaging initial time, respectively. It can be observed that the required synthetic aperture time is related to the target characteristics such as the speed \mathbf{V}_j and the initial relative position \mathbf{R}_{OT} between the radar and the targets. Once the target characteristics are obtained by conventional tracking algorithms [19], the required synthetic aperture time can be calculated according to the formula (6). Thus, the target characteristics also affect the azimuth resolution and the section of the radars to image the targets.

In addition, ISAR imaging requires long-term continuous observation to maintain a sufficiently high-resolution image if traditional Range-Doppler algorithm is used. After careful analysis and experiment, the scattered model is applied to describe the target in the ISAR imaging scene. Then, the energy of the radar echo is composed of several strong and dominant scattering points. According to the sparsity of the target, an ISAR image can be reconstructed with sparse imaging algorithms based on Compressed Sensing theory [3–5], which can reconstruct a signal with far fewer measurements. The slow time echo $S_r(f, m)$, $m = 1, \dots, M_{all}$ can be considered as sparse in the azimuth domain, where M_{all} represents the number of the whole pulses transmitted during the synthetic aperture time. The observation pulses of a target are randomly selected by a sparse observation matrix during the synthetic aperture time, as illustrated in Fig. 5. Then, through a small amount and random observation data $S_r(f, m)$, $m = 1, \dots, M_s$ where $M_s < M_{all}$, the original slow time echo can be reconstructed by Orthogonal Matching Pursuit (OMP) algorithm [20]. Consequently, the ISAR image is obtained by solving a sparsity-constrained optimization problem.

Obviously, through alternate observation with fewer observation pulses, an ISAR image is obtained successfully. Meanwhile, the unoccupied pulses are used to image



other targets. Notably, the synthetic aperture time required for imaging is not changed, while the number of observation pulses is greatly reduced. Thus, the sparse imaging algorithm brings high degree of freedom in task scheduling problem.

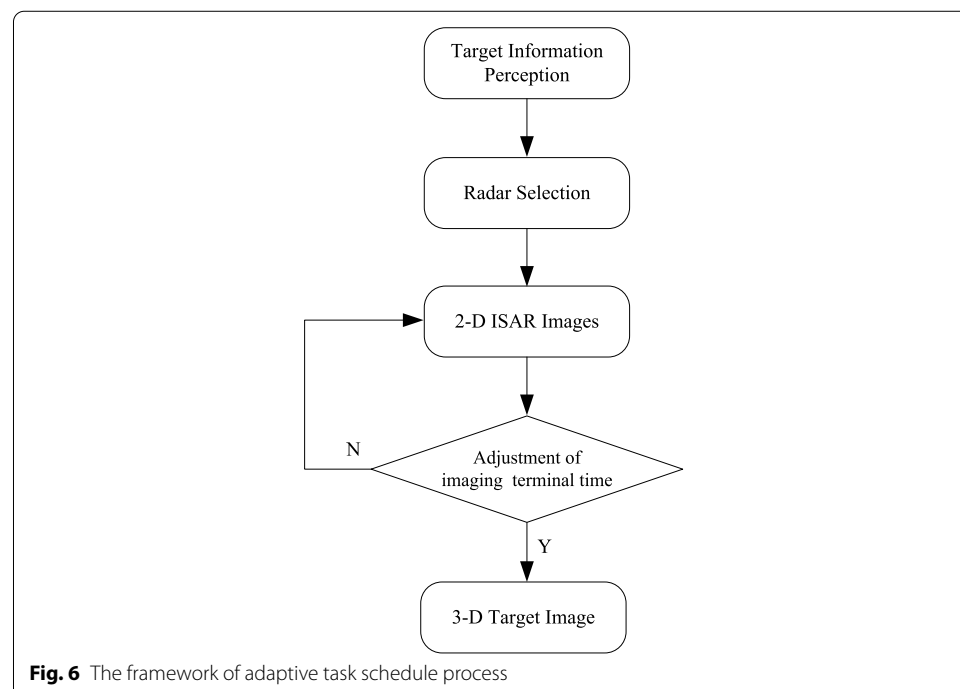
Therefore, combined with sparse imaging algorithms, the task scheduling problem can be established, while the quality of the 3-D target image is guaranteed and the minimal task time is used.

3 Methods

As mentioned above, a 3-D target image can be constructed by multiple-view observation information from different dispersed radars. To ensure the accuracy of 3-D target image, three independent and non-collinear radars are usually selected to image one target simultaneously. In a nutshell, a 3-D target image will be achieved when three different ISAR images are obtained.

The targets characteristics such as the speed and the distance will also affect the task schedule strategy and the image quality. Obviously, the effective way to allocate radar resources is to do it adaptively combined with the target characteristics. The sparse ISAR imaging algorithm [4] which makes cognitive imaging possible is adopted in the adaptive task scheduling strategy. Then, the brief task scheduling process is depicted in Fig. 6, where there are three key parts.

Target Information Perception: Task allocation is closely related to the target characteristics, thus target information perception is the prerequisite for task scheduling optimization problem. The target characteristics such as the distance, the speed, the size, the sparsity, and the imaging resource requirements can be cognized by transmitting a small number of pulses first.



Radar selection: After the imaging resource requirements of each target is obtained, the radar selection module can obtain an approximate optimal solution to finish the whole imaging tasks using the minimal task time.

Adjustment of imaging terminal time: The imaging accumulation time of each target can be adjusted by the closed-loop feedback between the receiver and the transmitter. To be specific, the imaging terminal time can be adaptively adjusted according to the comparison of the ISAR image quality between the adjacent scheduling intervals. Thus, the utilization of radar resources can be further improved.

The three key parts will be described in detail in the upcoming subsection.

3.1 Target information perception

A few pulses are transmitted by each radar and the target characteristics can be cognitive obtained by the echo signal.

First, through tracking processing, the basic characteristics such as the speed V^j , the heading θ^j , the priority P^{ij} of the j th target, and the distance R^{ij} between the i th radar and the j th target can be measured [19]. Thereafter, the sparsity K^{ij} of the j th target corresponding to the i th radar can be calculated according to the coarse-resolution ISAR image. Furthermore, the measurement dimension M^{ij} (i.e., the required observation pulses) can be reckoned by

$$M^{ij} \geq c_1 K^{ij} \ln(T_c^{ij} \cdot PRF_i) \quad (8)$$

where T_c^{ij} denotes the required synthetic aperture time, which depends on the expected azimuth resolution ρ_a^j as analyzed in formula (2). PRF_i denotes the pulse repetition rate of the i th radar.

Furthermore, the measure dimension of each scheduling interval M_{per}^{ij} is determined by

$$M_{per}^{ij} = \frac{M^{ij}}{T_c^{ij} / T_0} \quad (9)$$

where T_0 denotes the time of scheduling interval.

When the measurement dimension meets the condition (8)–(9), the radar observation resources required for each target are known, thus the radar selection optimization model can be established in upcoming section.

3.2 Radar selection optimization

As mentioned above, the imaging time (i.e., the synthetic aperture time) for each target is closely related to the required azimuth resolution, the relative position of the radars and the targets, and the target characteristics. Once the required azimuth resolution and the target characteristics are determined as a prior information, the selection of the radars to image the targets is necessary and needs to be optimized.

Note that, three independent and non-collinear radars are usually selected to image one target simultaneously to construct the 3-D target image. Combined with sparse ISAR imaging algorithm, each radar can image multiple targets by alternate observation. Consequently, the optimization model is established as

$$\begin{aligned}
& \text{minimize } \max(\mathbf{A} \cdot \mathbf{X}) \\
& \text{s.t. } \begin{cases} \mathbf{X}(i, j) \in \{0, 1\} \\ \sum_{i=1}^M \sum_{j=1}^N \mathbf{X}(i, j) = 3N \\ \sum_{i=1}^M \mathbf{X}(i, j) = 3, \forall j \in [1, n] \\ \sum_{j=1}^N \mathbf{X}(i, j) \cdot \mathbf{B}(i, j) \leq 1, \forall i \in [1, n] \\ i = 1, 2, \dots, M \\ j = 1, 2, \dots, N \end{cases} \quad (10)
\end{aligned}$$

where the $M \times N$ matrix \mathbf{X} denotes the radar selection strategy and each element in matrix \mathbf{X} can only take 0 or 1. $\mathbf{X}(i, j)=1$ represents the i th radar is chosen to image the j th target, otherwise not. Multiple radars may be assigned to a target to obtain a 3-D target image. Similarly, the $M \times N$ matrix \mathbf{A} represents the required synthetic aperture time of the corresponding radar selection strategy and each element can be determined by $\mathbf{A}(i, j)=t_{ij}$ based on formula (7). The total synthetic aperture time is determined by the longest synthetic aperture time among all the imaging tasks. Thus, the total synthetic aperture time for the overall imaging tasks in radar network is chosen as the objective function. Then, by minimizing the maximum of the Hadamard product of matrix \mathbf{A} and \mathbf{X} , the radar selection optimization model is formulated.

In addition, the fourth constrain in (10) should be satisfied by the targets which are imaged by the same radar. To be specific, we define the aperture occupancy ratio as the ratio of the pulses assigned to each target to the overall transmitted pluses of the radar in a scheduling interval. Then, the $M \times N$ matrix \mathbf{B} represents the aperture occupancy ratios in radar network and each element can be measured by

$$\mathbf{B}(i, j) = \frac{1}{\left\lfloor T_0 \cdot PRF_i / M_{per}^{i,j} \right\rfloor} \quad (11)$$

where the symbol $\lfloor \cdot \rfloor$ denotes the operation of round toward negative infinity.

Obviously, the radar selection optimization problem is a combinatorial optimization problem and non-convex because of the first constraint in formula (11) where the element in matrix \mathbf{X} can only take 0 or 1 (i.e., $\mathbf{X}(i, j) \in \{0, 1\}$). Thus, it is a challenge to obtain an optimal radar selection strategy.

To deal with this problem, we try to turn it to a convex optimization problem by choosing convex relaxation methods [21–23]. Thus, the radar selection optimization model is reformulated as

$$\begin{aligned}
& \text{minimize } \max (\mathbf{A} \cdot \mathbf{X}) \\
& \text{s.t. } \begin{cases} 0 \leq \mathbf{X}'(i, j) \leq 1 \\ \sum_{i=1}^M \sum_{j=1}^N \mathbf{X}'(i, j) = 3N \\ \sum_{i=1}^M \mathbf{X}'(i, j) = 3, \forall j \in [1, n] \\ \sum_{j=1}^N \mathbf{X}'(i, j) \cdot \mathbf{B}(i, j) \leq 1, \forall i \in [1, n] \\ i = 1, 2, \dots, M \\ j = 1, 2, \dots, N \end{cases} \quad (12)
\end{aligned}$$

First, we relax the constraint by introducing a weight matrix \mathbf{X}' where the elements range from 0 to 1 to replace the original matrix \mathbf{X} . Then, the weight matrix \mathbf{X}' can be obtained by using the CVX toolbox. For each column in the matrix \mathbf{X}' , it is known that the greater the value in a row, the larger the weight assigned to the corresponding radar. Then, the selection matrix \mathbf{X} can be easily obtained by letting the first three larger values of each column in weight matrix \mathbf{X}' be 1, while letting the others be 0. If the fourth constraint in formula (11) is not satisfied as expected, the former selection matrix \mathbf{X} can be used as the input matrix to the optimization model. Through iterative processing, the selection matrix \mathbf{X} can be finally obtained.

Sometimes it is not possible to schedule all the targets at the same time according to the proposed optimization model due to resource constraints. Then, it is necessary to analyze the range of number of targets N_O that the radar selection model can optimize simultaneously. The maximum number N_{\max} , which is determined by the sum of the minimum aperture occupancy ratios, can be calculated by

$$N_{\max} = \max \left\{ x \left| \sum_{j=1}^x \min (\mathbf{B}(:, j)) \leq M \right. \right\} \quad (13)$$

Similarly, the minimum number N_{\min} , which is determined by the sum of the maximum aperture occupancy ratios, can be calculated by

$$N_{\min} = \max \left\{ x \left| \sum_{j=1}^x \max (\mathbf{B}(:, j)) \leq M \right. \right\} \quad (14)$$

Then, the number of targets N_O that can optimize is determined by $N_{\min} \leq N_O \leq N_{\max}$.

Through the analysis, it is observed that if the equality $N_{\min} = N = N_{\max}$ holds, all the targets can be scheduled simultaneously by the proposed optimization model. If the inequality $N \geq N_{\min}$ holds, it is unlikely that all the targets can be scheduled at the same time. Generally, N_{\min} targets are chosen first to the radar selection model according to the priority. When the imaging task is accomplished, the corresponding radar resources are free and the following targets can be executed in succession according to the priority and the radar resource constraints.

3.3 The adjustment of imaging terminal time

Generally speaking, the ISAR image quality should increase with the increase in the synthetic aperture time, until it comes to a standstill. Since then, the ISAR image quality will become worse even the synthetic aperture time increases. Therefore, the closed-loop feedback between the receiver and the transmitter can be used to adjust the synthetic aperture time of each target and the radar resource utilization can be further improved.

To be specific, the imaging terminal time can be adaptively adjusted according to the comparison of the ISAR images between scheduling intervals. The information entropy I is chosen as an indicator to measure the changes of ISAR images in this case. The information entropy of an ISAR image in the k th schedule interval I^k can be calculated by

$$I^k = -\sum p(a) \ln p(a) \quad (15)$$

where $p(a)$ represents the gray probability distributions of an ISAR image and is approximately evaluated by the statistical results of the gray histogram [24–26].

It is known that the smaller the information entropy, the higher the image quality. With the increase in synthetic aperture time, the information entropy will be decreased and the imaging quality will be improved. Then, in this case, we can continue to transmit pulses in the next scheduling interval to improve the image quality. While the image quality comes to a standstill, the changes of information entropy are relatively small, it is difficult and unnecessary to continue to transmit pulses to improve the image quality.

Then, an appropriate threshold Q_{th} is chosen to control this imaging process. In general, if the change of the information entropy between two adjacent schedule interval is less than ten percent of the previous information entropy, the change is relatively small and can be set as the threshold (i.e., $Q_{th} = (I^k - I^{k-1}) / 10$). Consequently, if the change of the information entropy is smaller than the threshold Q_{th} , the image quality is considered to reach the expected standard and the corresponding task is finished. Otherwise, the imaging task continues to execute in the next scheduling interval. The saved radar resources can be used to perform other tasks.

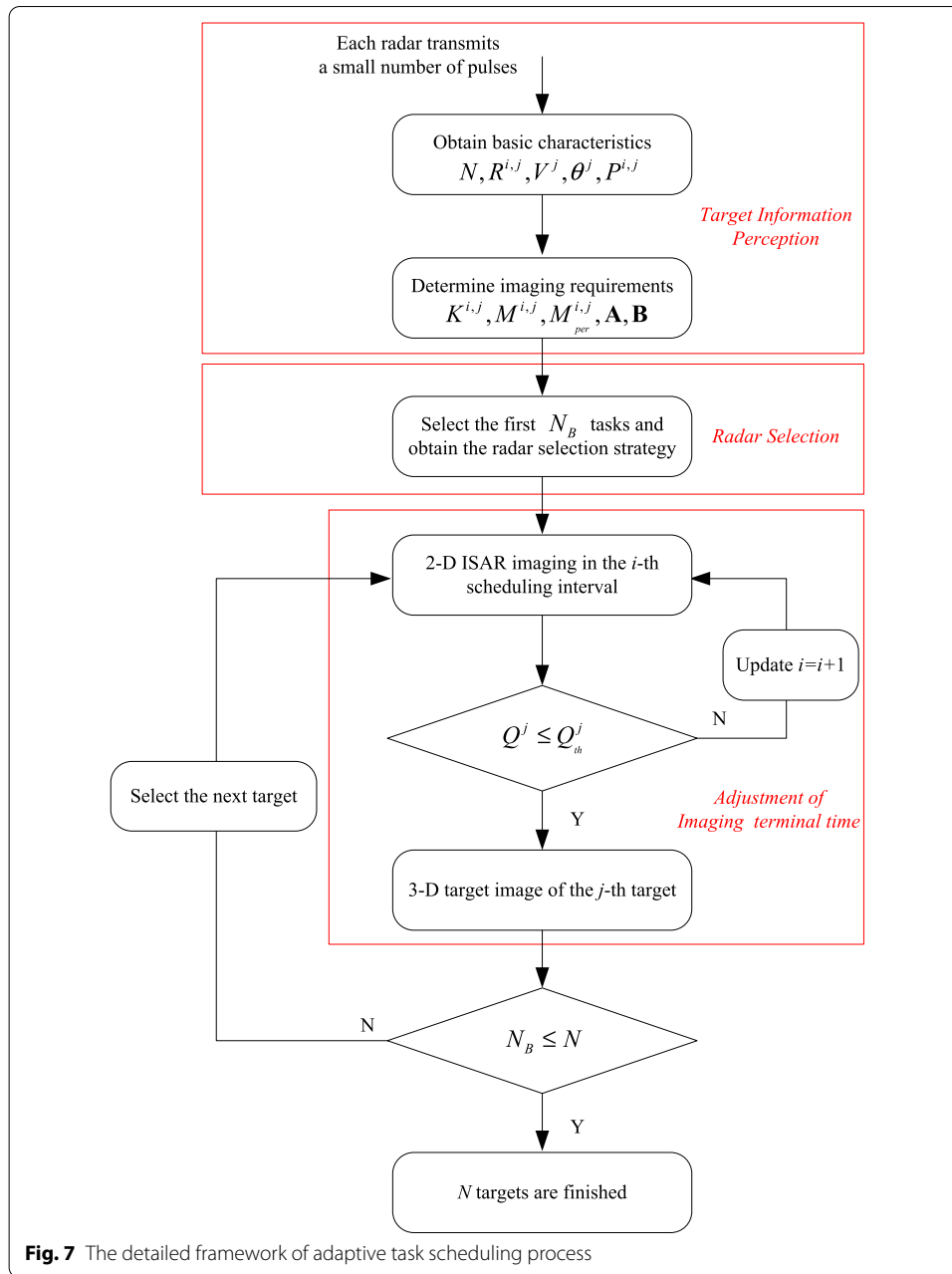
Once the three ISAR images of each target are finished, the 3-D target image is constructed smoothly.

In a nutshell, the concrete flow of the task scheduling method is depicted in Fig. 7. For better understanding, the detail steps of the proposed task scheduling strategy are also summarized as follows:

Step 1) A few pulses is transmitted to the targets by the radars in radar network and the target characteristics such as the distance R^{ij} , the speed V^j , the heading θ^j , the number of targets N , and the priority P^{ij} is cognized initially.

Step 2) Obtain the coarse ISAR image and determine the imaging resource requirements such as the sparsity K^{ij} , the measurement dimension M^{ij} and the measure dimension of each scheduling interval M_{per}^{ij} , the matrix of imaging time \mathbf{A} , the matrix of aperture occupancy ratio matrix \mathbf{B} .

Step 3) Select the first N_B targets according to the priority, and allocate the imaging tasks including the M radars and N_B targets according to the optimization model in (9).



Step 4) Perform ISAR imaging tasks in current scheduling interval and calculate the change of the information entropy of ISAR images between adjacent scheduling intervals in radar network. When the changes of the information entropy Q are smaller than the preset threshold Q_{th} , the imaging terminal time is determined and the corresponding imaging task is finished. Otherwise, continue performing the corresponding imaging task in next scheduling interval.

Step 5) Update the resource utilization information of each radar in radar network and select the next and appropriate target according to radar resource requirements.

Step 6) Determine whether the overall imaging tasks are finished or not. If some imaging tasks are not finished, then go to step 4.

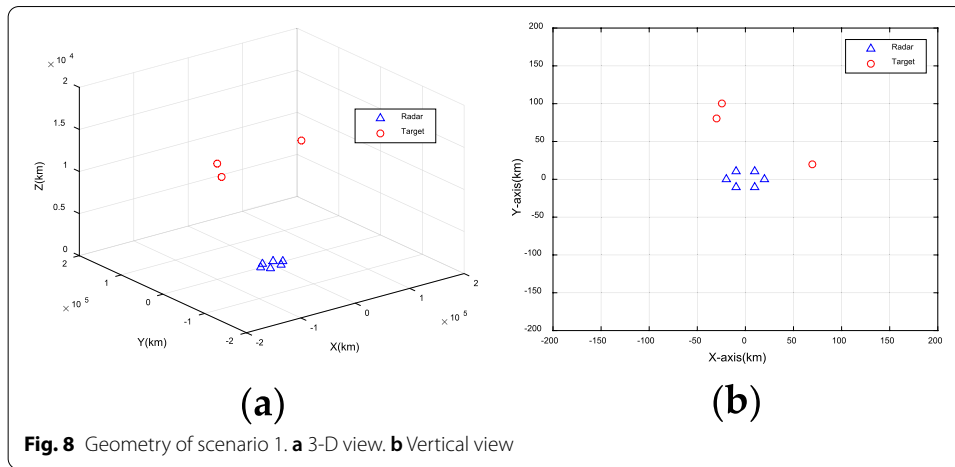


Fig. 8 Geometry of scenario 1. **a** 3-D view. **b** Vertical view

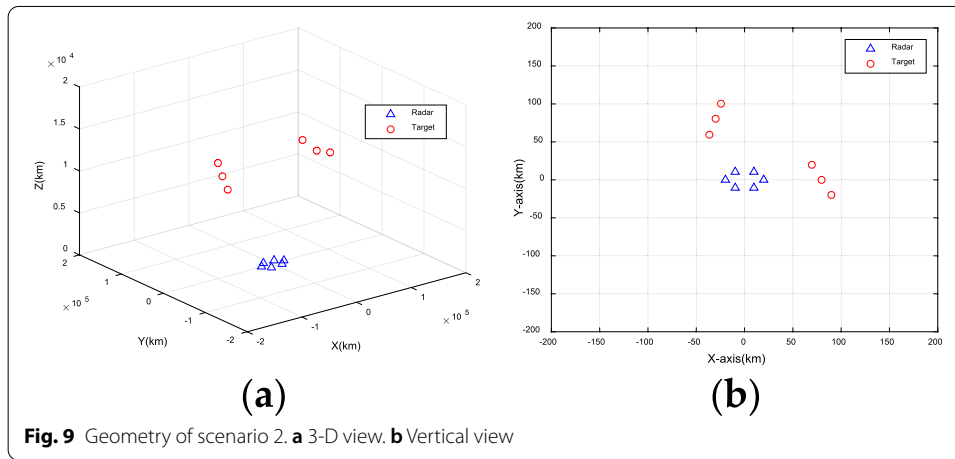


Fig. 9 Geometry of scenario 2. **a** 3-D view. **b** Vertical view

Step 7) Perform the 3-D target imaging according to formula (4) and the 3-D imaging tasks are done.

4 Results and discussion

Some experiments are performed to demonstrate the effectiveness of the proposed task scheduling strategy in realizing the multi-target 3-D imaging task while using the minimal task time in this section.

Assume that the radar network is constituted of six non-collinear homogeneous radars, and time synchronization has been realized between the radars. Two different scenarios with 3 and 6 targets, respectively, are set in this experiment, as shown in Figs. 8 and 9. Scenario 2 adds some targets on the basis of Scenario 1 to create a slightly resource-constrained situation. We assume that the radars have the same operating parameters. Linear frequency modulation (LFM) signal is applied for imaging tasks. The carrier frequency is 10 GHz, the pulse width is 1 μ s, the signal bandwidth is 300 MHz, the pulse repetition frequency is 1000 Hz and the scheduling interval is 1 s.

4.1 Task scheduling optimization

Each radar in radar network transmits a handful of pulses to cognize the target characteristics. Then, the distance, the coordinates, the speed, the heading, the priority can be evaluated by conventional tracking algorithm [19]. Furthermore, the coarse ISAR image can be reconstructed by matched filtering algorithm. Then, the sparsity, the measurement dimension and the aperture occupancy ratio can be calculated. For simplicity's sake, we consider the required azimuth resolution of each target is 1 m. The required target information of the two different scenarios are illustrated from Tables 1 to 2.

Based on the perception of target information, we can continue to complete the task scheduling work. The imaging time matrix \mathbf{A} of the two scenarios is calculated and illustrated as a histogram in Fig. 10. The proposed task scheduling method is applied to schedule the targets. Subsequently, as shown in Table 3, the optimal task scheduling strategy with minimal total synthetic aperture time is obtained. Meanwhile, the black arrows represent the selection of radars (i.e., radar selection strategy) and the red arrow indicates the total task time, as shown in Fig. 10.

Table 1 Characteristics of the targets in scenario 1

Targets	Coordinates (km)	Velocity (m/s)	Aperture occupancy ratio
Target 1	(70, 20, 13.1)	(400, −200, 0)	1/3, 1/3, 1/3, 1/4, 1/4, 1/3
Target 2	(−30, 80, 9.1)	(−100, −500, 0)	1/4, 1/4, 1/3, 1/4, 1/3, 1/3
Target 3	(−24, 100, 10.1)	(−100, −500, 0)	1/3, 1/3, 1/4, 1/3, 1/4, 1/3

Table 2 Characteristics of the targets in scenario 2

Targets	Coordinates (km)	Velocity (m/s)	Aperture occupancy ratio
Target 1	(70, 20, 13.1)	(−400, −200, 0)	1/3, 1/3, 1/3, 1/4, 1/4, 1/3
Target 2	(80, 0, 12.1)	(−400, −200, 0)	1/3, 1/4, 1/3, 1/4, 1/3, 1/3
Target 3	(90, −20, 12.1)	(−400, −200, 0)	1/3, 1/3, 1/4, 1/3, 1/4, 1/3
Target 4	(−36, 60, 8.1)	(−100, −500, 0)	1/3, 1/4, 1/3, 1/3, 1/4, 1/3
Target 5	(−30, 80, 9.1)	(−100, −500, 0)	1/3, 1/3, 1/3, 1/4, 1/3, 1/3
Target 6	(−24, 100, 10.1)	(−100, −500, 0)	1/3, 1/4, 1/3, 1/3, 1/3, 1/4

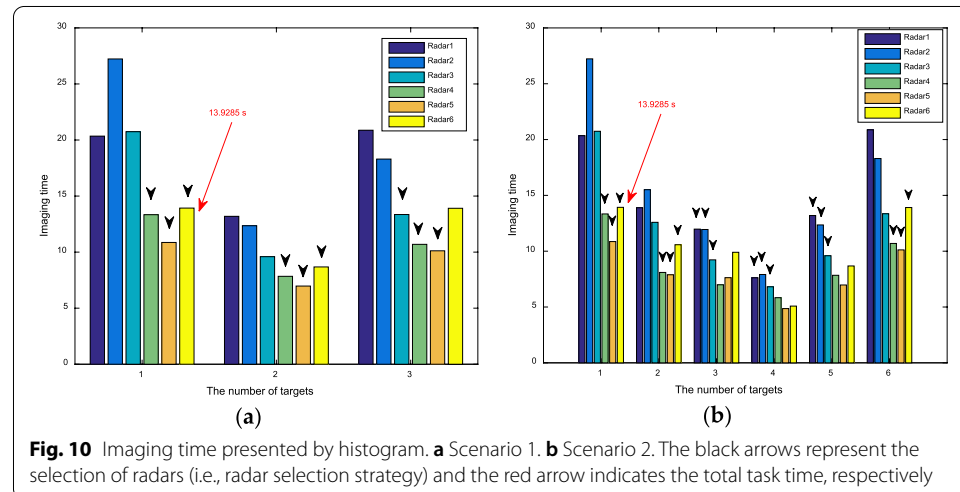
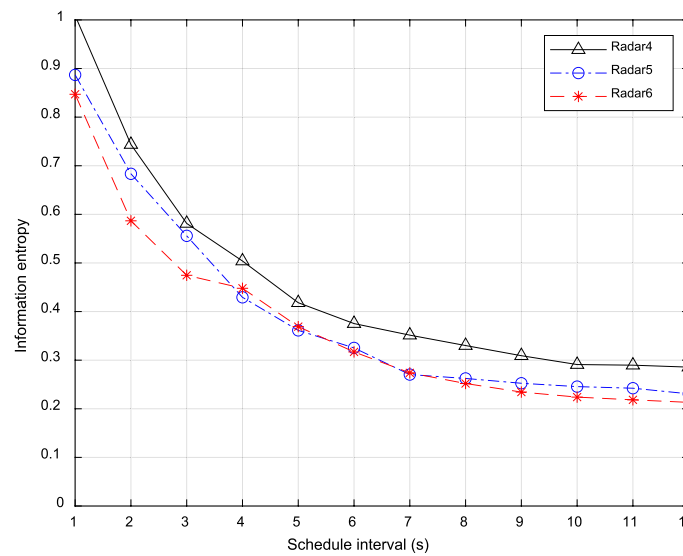


Table 3 The optimal radar selection scheme

Scenarios	Targets	Radar selection
Scenario 1	Target 1	Radar 4, 5, 6
	Target 2	Radar 4, 5, 6
	Target 3	Radar 3, 4, 5
Scenario 2	Target 1	Radar 4, 5, 6
	Target 2	Radar 4, 5, 6
	Target 3	Radar 1, 2, 3
	Target 4	Radar 1, 2, 3
	Target 5	Radar 1, 2, 3
	Target 6	Radar 4, 5, 6

**Fig. 11** The curve of the information entropy for Target 6

Note that, in the scenario 1, the radars assigned to each target are those with the minimal imaging time and there are still free radars exist. This is because the radar resources are relatively abundant at this time, the optimal radar selection strategy for each target can be obtained. As the number of targets increases, the conflicts in radar resources appeared. As shown in Fig. 10b, the radars assigned to Target 4 are not those with the minimal imaging time (i.e., the radars assigned are not individually optimal). But for the overall imaging task, the minimal total task time is obtained with the radar selection strategy. In a conclusion, when the radar resources are tight, the imaging time of individual target will be sacrificed to achieve overall optimization.

Furthermore, the imaging terminal time can be adjusted according to the changes of the information entropy between the adjacent scheduling intervals. For instance, the curve of the information entropy of Target 6 in scenario 2 is shown in Fig. 11. It can be observed that as the synthetic aperture time increases, the information entropy decreases and the image quality improves correspondingly at the beginning. Subsequently, the curve of the information entropy will tend to be stable and the change of

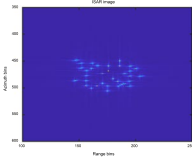
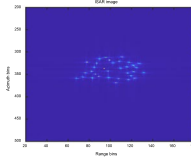
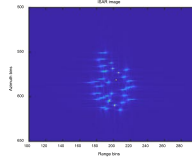
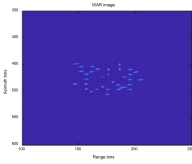
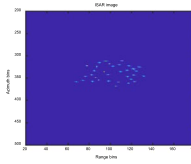
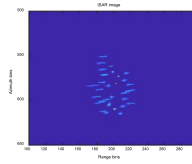
the information entropy is smaller than the threshold Q_{th} . This means that the ISAR images between the adjacent scheduling intervals are highly similar and the image quality is hard to improve. Thus, the imaging terminal time can be determined and the corresponding imaging task is early finished compared with a pre-calculated time. Through the dynamic adjustment of imaging terminal time, the saved radar resource can be used to perform other tasks and the resource utilization is further improved.

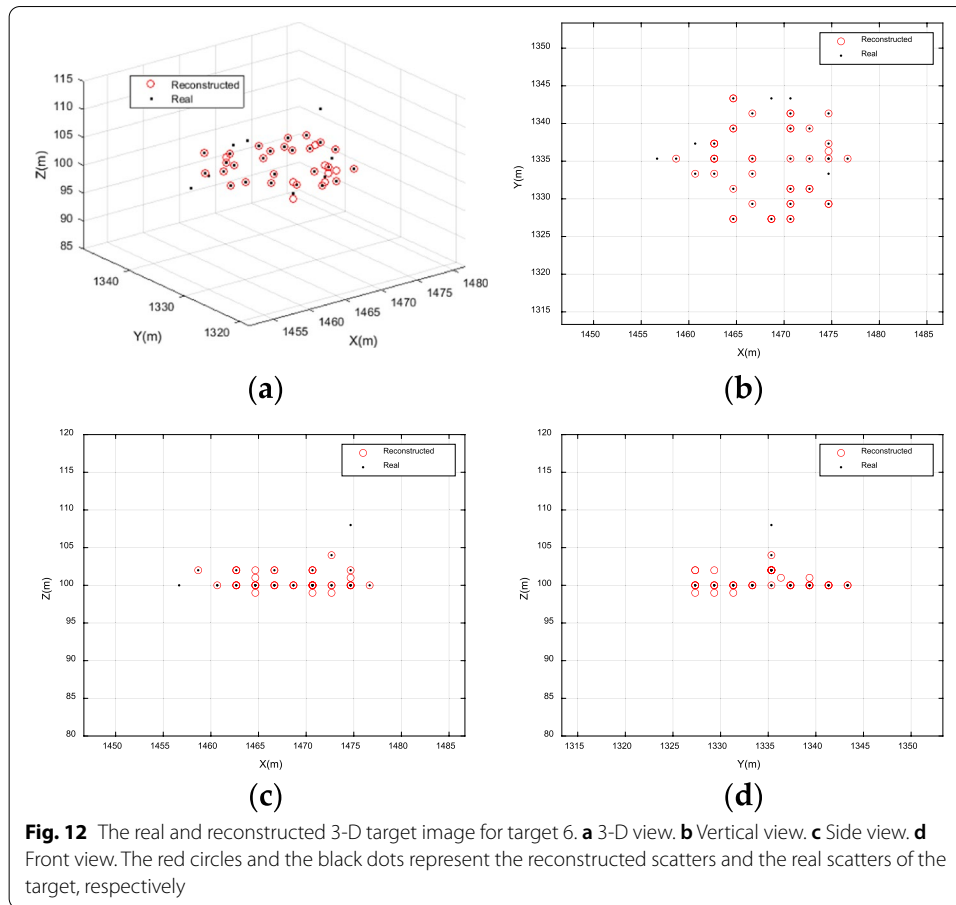
4.2 Image performance

Different with the traditional Range-Doppler algorithm, the CS-based sparse imaging algorithm makes a high-resolution ISAR image possible with a handful of random discontinuous observation pulses. The reduced observation pluses can be applied to image other targets simultaneously. Thus, the flexibility for radar resource allocation can be expanded and the radar resource utilization can be improved. In order to measure the image quality of ISAR images using CS-based algorithm, we conducted a comparative experiment with Range-Doppler algorithm which uses full observation pulses during the synthetic aperture time. As described in Table 4, the correlation coefficients of the ISAR images of the same target using different imaging algorithms are 0.9533, 0.9655 and 0.9685, respectively. Consequently, the ISAR images with the CS-based sparse imaging algorithm are similar to those with traditional imaging algorithm [27–30].

Based on the three ISAR images of the Target 6, a 3-D target image can be constructed subsequently. The reconstructed 3-D image result is illustrated in Fig. 12a and the top, front and side views of the 3-D image are presented in Fig. 12b–d, respectively. The black dots represent the real scatters of the target and the red circles represent the reconstructed scatters. It can be observed that the positions of the reconstructed scatters are very close to those of the real target model. In fact, how to further reduce the errors of 3-D reconstructed image is worth studying, while the focus of this article is on task scheduling rather than imaging algorithms.

Table 4 Image comparison of different imaging algorithms

	Radar 4	Radar 5	Radar 6
Traditional ISAR imaging			
Sparse aperture ISAR imaging			
Correlation coefficient	0.9533	0.9655	0.9685



Therefore, through reasonable and effective task scheduling method, the multiple 3-D target image can be accomplished efficiently.

5 Conclusions

This article presents an adaptive multi-target task scheduling algorithm for 3-D target imaging in radar network. Combined with multi-view ISAR imaging results, a 3-D image of the target can be constructed. Moreover, the CS-based sparse imaging algorithm is introduced to obtain the ISAR images of each target, which also brings high degree of freedom to radar task scheduling. After the target information perception, the radar selection problem which is a discrete optimization problem can be solved by relaxed convex optimization algorithm. In addition, the imaging terminal time can be adjusted adaptively based on the information entropy of the adjacent ISAR images. Through the steps of target information perception, radar selection and adaptive adjustment of imaging terminal time, we achieved the multi-target 3-D imaging task with the minimal total task time. Finally, simulation results show that the proposed task scheduling algorithm is effective and the radar resource utilization is significantly improved. As a preliminary attempt, the proposed task scheduling method only takes the radar time resource into consideration nevertheless. There are some other resources such as power and waveform resources that deserve future research.

Abbreviations

ISAR: Inverse synthetic aperture radar; CS: Compressed sensing; 2-D: Two dimensional; 3-D: Three dimensional; IPP: Imaging projection plane.

Acknowledgements

The authors would like to thank the handling editor and the anonymous reviewers for their valuable comments and suggestions for this paper. This work was supported in part by the National Natural Science Foundation of China Grant Numbers 62131020, 61971434.

Authors' information

Dan Wang was born in Anhui, China, in 1990. He is currently pursuing the Ph.D. degree in electrical engineering from the Institute of Information and Navigation, Air Force Engineering University (AFEU), Xi'an, China. His current research interests include signal processing and radar imaging. Qun Zhang and Ying Luo are professors in the Institute of Information and Navigation, Air Force Engineering University (AFEU), Xi'an, China. Their research interests include signal processing, clutter suppression, and its application in SAR and ISAR. Xiao-wen Liu is currently working in School of Information and Communications, National University of Defense Technology, Xi'an, China. His current research interests include signal processing and radar imaging. Jia Liang was born in Shaanxi, China, in 1985. He is currently pursuing the Ph. D. degree in signal and information processing. His research interests include array radar signal processing and target feature extraction and recognition.

Author contributions

DW and QZ proposed the method and designed the experiments; DW performed the experiments and wrote; QZ, YL, XL, and JL revised the paper. All authors read and approved the final manuscript.

Funding

This research was funded by the National Natural Science Foundation of China, Grant Numbers 62131020, 61971434.

Availability of data and materials

Please contact author for data requests.

Declarations

Ethics approval and consent to participate

Not applicable.

Consent for publication

The picture materials quoted in this article have no copyright requirements, and the source has been indicated.

Competing interests

The authors declare no competing interests.

Author details

¹The Institute of Information and Navigation, Air Force Engineering University, Xi'an 710077, China. ²The Key Laboratory for Information Science of Electromagnetic Waves (Ministry of Education), Fudan University, Shanghai 200433, China.

³The School of Information and Communications, National University of Defense Technology, Xi'an 710100, China.

Received: 4 February 2022 Accepted: 27 March 2022

Published online: 08 April 2022

References

1. M.A. Richards, *Fundamentals of Radar Signal Processing*, 2nd edn. (McGraw-Hill, New York, 2014)
2. D.A. Ausherman, A. Kozma, J.L. Walker et al., Developments in radar imaging. *IEEE Trans. Aerosp. Electron. Syst.* **AES-20**(4), 363–400 (2008)
3. X. Bai, G. Wang, S. Liu, F. Zhou, High-resolution radar imaging in low SNR environments based on expectation propagation. *IEEE Trans. Geosci. Remote Sens.* **59**(2), 1275–1284 (2021). <https://doi.org/10.1109/TGRS.2020.3004006>
4. L. Zhang, M.D. Xing, C.W. Qiu et al., Achieving higher resolution ISAR imaging with limited pulses via compressed sampling. *IEEE Geosci. Remote Sens. Lett.* **6**(3), 567–571 (2009)
5. D.L. Donoho, Compressed sensing. *IEEE Trans. Inf. Theory* **52**(4), 1289–1306 (2006)
6. X. Zhou, Y. Wang, C. Yeh, X. Lu, Recession parameter estimation from wideband measurements for 3-D ISAR imaging of cone-shaped targets. *IEEE Trans. Geosci. Remote Sens.* **19**, 1–5 (2022). <https://doi.org/10.1109/LGRS.2021.3129740>
7. L. Liu, Z. Zhou, F. Zhou, X. Shi, New 3-D geometry reconstruction method of space target utilizing the scatterer energy accumulation of ISAR image sequence. *IEEE Trans. Geosci. Remote Sens.* **58**(12), 8345–8357 (2020). <https://doi.org/10.1109/TGRS.2020.2986465>
8. X. Bai, Z. Bao, High-resolution 3D imaging of precession cone-shaped targets. *IEEE Trans. Antennas Propag.* **62**(8), 4209–4219 (2014)
9. X.-W. Liu, Y.-F. Qun Zhang, Y.-C. Yin, F. Zhu, Three-dimensional ISAR image reconstruction technique based on radar network. *Int. J. Remote Sens.* **41**(14), 5399–5428 (2020). <https://doi.org/10.1080/01431161.2020.1731932>

10. J. Yan, W. Pu, S. Zhou, H. Liu, Z. Bao, Collaborative detection and power allocation framework for target tracking in multiple radar system. *Inf. Fusion* **55**, 173–183 (2020)
11. J. Yan, J. Dai, W. Pu, S. Zhou, H. Liu, Z. Bao, Quality of service constrained-resource allocation scheme for multiple target tracking in radar sensor network. *IEEE Syst. J.* **15**(1), 771–779 (2021)
12. T. Tian, T. Zhang, L. Kong, Timeliness constrained task scheduling for multifunction radar network. *IEEE Sens. J.* **19**(2), 525–534 (2019). <https://doi.org/10.1109/JSEN.2018.2878795>
13. T. Zhang, J. Liang, Y. Yang et al., Antenna deployment method for multistatic radar under the situation of multiple regions for interference. *Signal Process.* **143**, 292–297 (2018)
14. A. Deligiannis, A. Panoui, S. Lambotharan, J.A. Chmiers, Game-theoretic power allocation and the Nash Equilibrium analysis for a multistatic MIMO radar network. *IEEE Trans. Signal Process.* **65**(24), 6397–6408 (2017)
15. H. Zhang, W. Liu, B. Zong, J. Shi, J. Xie, An efficient power allocation strategy for maneuvering target tracking in cognitive MIMO radar. *IEEE Trans. Signal Process.* **69**, 1591–1602 (2021). <https://doi.org/10.1109/TSP.2020.3047227>
16. H. Zhang, J. Xie, J. Shi, T. Fei, J. Ge, Z. Zhang, Joint beam and waveform selection for the MIMO radar target tracking. *Signal Process.* **156**, 31–40 (2019)
17. D. Wang, K.-M. Li, Q. Zhang, X.-F. Lu, Y. Luo, A cooperative task allocation game for multi-target imaging in radar networks. *IEEE Sens. J.* **21**(6), 7541–7550 (2021)
18. D. Wang, Q. Zhang, Y. Luo, X. Liu, J. Ni, L. Su, Joint optimization of time and aperture resource allocation strategy for multi-target ISAR imaging in radar sensor network. *IEEE Sens. J.* **21**(17), 19570–19581 (2021). <https://doi.org/10.1109/JSEN.2021.3090053>
19. Y.J. Chen, Q. Zhang, N. Yuan et al., An adaptive ISAR-imaging-considered task scheduling algorithm for multi-function phased array radars. *IEEE Trans. Signal Process.* **63**(19), 5096–5110 (2015)
20. L. Zhang et al., Resolution enhancement for inversed synthetic aperture radar imaging under low SNR via improved compressive sensing. *IEEE Trans. Geosci. Remote Sens.* **48**(10), 3824–3838 (2010)
21. M. Grant, S. Boyd. CVX: MATLAB Software for Disciplined Convex Programming (2008). <http://stanford.edu/~boyd/cvx>
22. S. Joshi, S. Boyd, Sensor selection via convex optimization. *IEEE Trans. Signal Process.* **57**(2), 451–462 (2009)
23. S. Boyd, L. Vandenberghe, *Convex Optimization* (Cambridge Univ. Press, New York, 2004)
24. J.-H. Han, S. Yang, B.-U. Lee, A novel 3-D color histogram equalization method with uniform 1-D gray scale Histogram. *IEEE Trans. Image Process.* **20**(2), 506–512 (2011). <https://doi.org/10.1109/TIP.2010.2068555>
25. Y. Du, K.-F. Liao, S. Ouyang, J.-J. Li, G.-J. Huang, Time and aperture resource allocation strategy for multitarget ISAR imaging in a radar network. *IEEE Sens. J.* **20**(6), 3196–3206 (2020)
26. C. Shi, L. Ding, F. Wang, S. Salous, J. Zhou, Joint target assignment and resource optimization framework for multitarget tracking in phased array radar network. *IEEE Syst. J.* **15**(3), 4379–4390 (2021). <https://doi.org/10.1109/JSYST.2020.3025867>
27. L. Liu, F. Zhou, M. Tao, P. Sun, Z. Zhang, Adaptive Translational Motion Compensation Method for ISAR Imaging under SNR Based on Particle Swarm Optimization. *IEEE J. Sel. Top. Appl. Earth Obs. Remote Sens.* **8**(11), 5146–5157 (2015)
28. X. He, N. Tong, X. Hu, High-resolution imaging and 3-D reconstruction of precession targets by exploiting sparse apertures. *IEEE Trans. Aerosp. Electron. Syst.* **53**(3), 1212–1220 (2017)
29. S. Zhang, Y. Liu, X. Li, D. Hu, Enhancing ISAR image efficiently via convolutional reweighted L1 minimization. *IEEE Trans. Image Process.* **30**, 4291–4304 (2021)
30. S. Ding, N. Tong, Y. Zhang, X. Hu, X. Zhao, Cognitive antenna selection in MIMO imaging radar. *IEEE Trans. Geosci. Remote Sens.* **59**(12), 9829–9841 (2021)

Publisher's Note

Springer Nature remains neutral with regard to jurisdictional claims in published maps and institutional affiliations.

Submit your manuscript to a SpringerOpen[®] journal and benefit from:

- Convenient online submission
- Rigorous peer review
- Open access: articles freely available online
- High visibility within the field
- Retaining the copyright to your article

Submit your next manuscript at ► [springeropen.com](https://www.springeropen.com)